# Infrared Spectra and Density Functional Calculations of Small Vanadium and Titanium Carbonyl Molecules and Anions in Solid Neon

**Mingfei Zhou and Lester Andrews***

*Department of Chemistry, University of Virginia, Charlottesville, Virginia 22901*

*Received: February 15, 1999; In Final Form: May 4, 1999*

Laser-ablated vanadium and titanium atoms were reacted with CO molecules during condensation in excess neon. The $V(CO)_x$ and $Ti(CO)_x$ ($x = 1-6$) molecules are formed during deposition or on annealing and photolysis. The $V(CO)_x^-$, $Ti(CO)_x^-$ ($x = 1-6$) anions and $TiCO^+$ cation are also produced and identified on the basis of isotopic substitution and density functional calculations. Selective photolysis and $CCl_4$ doping experiments strongly support the identification of the anions and cation.

## Introduction

Coordinatively unsaturated transition metal carbonyls are active species in catalytic reactions, and these molecules have been the focus of extensive and continuous study.[1] The $V(CO)_x$ complexes ($x = 1-5$) were produced by thermal V atom reactions with CO and infrared spectra were observed in solid rare gas matrixes.[2] Morton and Preston reported an electron spin resonance (ESR) study of $V(CO)_4$ and $V(CO)_5$ in a krypton matrix produced by gamma-irradiation of $V(CO)_6$.[3] Van Zee and co-workers prepared $V(CO)_x$ ($x = 1-3$) by co-condensing vanadium atoms with CO in excess rare gas and obtained ESR spectra.[4] A time-resolved infrared study of gas-phase $V(CO)_x$ ($x = 3-5$) produced by excimer laser photolysis of $V(CO)_6$ found some disagreement with matrix infrared and ESR studies.[5] The $V(CO)_6^-$ anion was produced by vacuum-ultraviolet irradiation of $V(CO)_6$ in solid argon.[6] More recently, the bond strengths of $V(CO)_x^-$ ($x = 3-6$) were determined by energy-resolved collision-induced dissociation of vanadium carbonyl anions in gas phase.[7] For titanium, the experimental data are very sparse. Binding energies of $Ti(CO)_x$ compounds were determined by chemiluminescence spectroscopy,[8] and the infrared spectrum of the saturated molecule $Ti(CO)_6$ in CO, Ar, Kr, and Xe matrixes was reported.[9] More recently, reactions of laser-ablated titanium atoms and oxides with CO in solid argon were studied in this laboratory, and infrared spectra of several titanium carbonyls were reported.[10]

Earlier extended Huckel calculations provided predictions of the geometries and spin multiplicities of the large $M(CO)_x$ ($x = 3-5$) species.[11,12] Bauschlicher and co-workers provided detailed ab initio calculations of the mono- and dicarbonyl neutrals as well as cations.[13,14] The monocarbonyls were also investigated by more recent density functional theory (DFT) calculations.[15−17]

Recent pulsed laser-ablation matrix isolation studies on later first-row transition metal and CO systems showed that, in contrast to thermal atom sources, metal cations and electrons are produced in the laser-ablation process, and as a result, molecular anions can be formed via electron capture by neutral molecules and molecular cations can be produced by metal cation reactions or ionization of neutral molecules during matrix condensation.[18−20] It is noteworthy that DFT frequency calculations and experiments find the C−O stretching modes for $FeCO^+ > FeCO > FeCO^-$ with large diagnostic 150−170 $cm^{-1}$ separations.[17,18] In this paper, we report the reactions of laser-ablated titanium and vanadium with CO in excess neon and argon. We will show that in addition to neutral carbonyls, carbonyl anions and cations are also produced and trapped in the matrix and identified by isotopic substitution and density functional calculations.

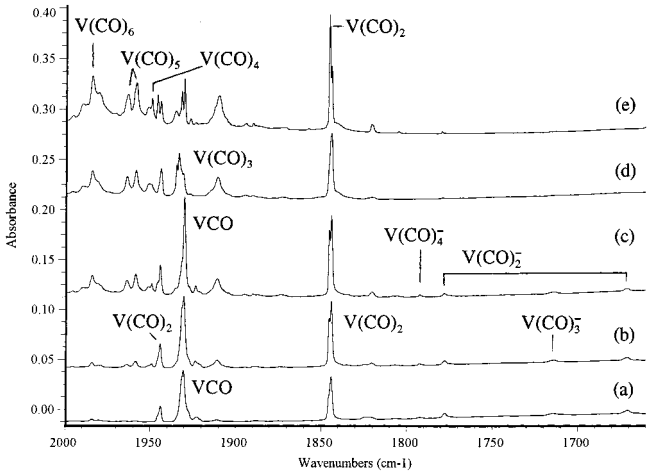


**Figure 1.** Infrared spectra in the 2000−1660 $cm^{-1}$ region from laser-ablated V atoms co-deposited with 0.1%CO in neon: (a) 30 min sample deposition at 4 K, (b) after annealing to 8 K, (c) after annealing to 10 K, (d) after 15 min full arc photolysis, and (e) after annealing to 10 K.

## Experimental Section

The experiment for laser ablation and matrix isolation spectroscopy was described in detail previously.[21−24] Briefly, the Nd:YAG laser fundamental (1064 nm, 10 Hz repetition rate with 10 ns pulse width) was focused on the rotating metal target (vanadium metal, Alfa, 99.5%; titanium metal, Goodfellow, 99.6%) using low energy (1−5 mJ/pulse). Laser-ablated metal atoms were co-deposited with carbon monoxide (0.05 to 0.5%) in excess argon or neon onto a 10 or 4 K CsI cryogenic window at 2−4 mmol/h for 1−2 h. Carbon monoxide (Matheson), isotopic $^{13}C^{16}O$ and $^{12}C^{18}O$ (Cambridge Isotopic Laboratories), and selected mixtures were used in different experiments. FTIR spectra were recorded at 0.5 $cm^{-1}$ resolution on a Nicolet 750

* To whom correspondence should be addressed.

10.1021/jp990549o CCC: $18.00 
Published on Web 06/22/1999

**TABLE 1: Infrared Absorptions ($cm^{-1}$) from Co-deposition of Laser-Ablated V with Carbon Monoxide in Excess Neon at 4 K**

| $^{12}C^{16}O$ | $^{13}C^{16}O$ | $^{12}C^{18}O$ | $^{12}C^{16}O + {}^{13}C^{16}O$ | ratio (12/13) | ratio (16/18) | assignment |
|---|---|---|---|---|---|---|
| 2140.8 | 2093.6 | 2089.7 | | 1.0225 | 1.0245 | CO |
| 2006.3 | 1958.1 | 1965.4 | | 1.0246 | 1.0208 | ? |
| 1984.3 | 1940.5 | 1936.8 | | 1.0226 | 1.0245 | $V(CO)_6$ |
| 1963.4 | 1920.1 | 1917.0 | | 1.0226 | 1.0242 | $V(CO)_5$ |
| 1958.5 | 1915.7 | 1911.8 | | 1.0223 | 1.0244 | $V(CO)_5$ |
| 1949.3 | 1906.6 | | | 1.0224 | | $(V(CO)_4)$ |
| 1946.3 | 1901.7 | 1903.0 | | 1.0235 | 1.0228 | $V(CO)_2$ site |
| 1944.0 | 1899.7 | 1900.4 | 1943.9, 1926.4, 1899.6 | 1.0233 | 1.0229 | $V(CO)_2$ |
| 1933.4 | 1890.3 | | | 1.0228 | | VCO site |
| 1930.6 | 1887.5 | 1885.8 | 1931.3, 1887.5 | 1.0228 | 1.0238 | VCO |
| 1910.8 | 1869.0 | 1864.1 | | 1.0224 | 1.0251 | $V(CO)_3$ |
| 1873.1 | 1831.5 | 1829.4 | | 1.0227 | 1.0239 | $V(CO)_6^-$ |
| 1845.6 | 1804.0 | 1803.9 | 1845.5, 1820.2, 1803.9 | 1.0231 | 1.0231 | $V(CO)_2$ site |
| 1844.2 | 1802.7 | 1802.2 | 1844.2, 1819.3, 1802.6 | 1.0230 | 1.0233 | $V(CO)_2$ |
| 1835.1 | 1794.3 | 1791.3 | | 1.0227 | 1.0245 | $V(CO)_5^-$ |
| 1820.7 | 1779.8 | 1780.0 | 1820.7, 1779.7 | 1.0230 | 1.0229 | $V_xCO$ |
| 1806.7 | 1764.7 | 1766.3 | | 1.0238 | 1.0228 | $VCO^-$ |
| 1792.6 | 1752.4 | 1750.9 | | 1.0229 | 1.0238 | $V(CO)_4^-$ |
| 1779.6 | 1739.4 | | 1779.7, 1739.4 | 1.0231 | | $V_xCO$ |
| 1777.9 | 1737.3 | 1738.2 | 1777.8, 1761.1, 1737.1 | 1.0234 | 1.0228 | $V(CO)_2^-$ |
| 1775.3 | 1734.3 | | | 1.0236 | | $V(CO)_4^-$ |
| 1714.3 | 1674.4 | 1677.2 | 1714.6, 1697.5, 1685.4, 1674.4 | 1.0238 | 1.0221 | $V(CO)_3^-$ |
| 1670.6 | 1632.1 | 1633.3 | | 1.0236 | 1.0228 | $V(CO)_2^-$ |
| 1583.4 | 1548.5 | 1547.9 | 1583.4, 1548.5 | 1.0225 | 1.0229 | $V_x[CO]$ |
| 1516.2 | 1482.8 | 1480.4 | 1516.2, 1498.1, 1482.8 | 1.0225 | 1.0242 | $(CO)_2^-$ |
| 1477.9 | 1443.7 | 1447.0 | 1477.9, 1452.4, 1443.6 | 1.0237 | 1.0214 | $V_x[CO]_2$ |

spectrometer with 0.1 $cm^{-1}$ accuracy using a HgCdTe detector. Matrix samples were annealed at different temperatures, and selected samples were subjected to broadband photolysis by a medium-pressure mercury arc (Philips, 175W) with the globe removed.

## Results

Infrared spectra of V + CO and Ti + CO systems will be presented followed by density functional calculations of metal carbonyl product species.

**V + CO/Ne.** Figure 1 shows the spectra in the 2000−1660 $cm^{-1}$ region with 0.1% CO in neon, and the absorptions are listed in Table 1. The spectrum after deposition reveals sharp strong new bands at 1844.2, 1930.6, and 1944.0 $cm^{-1}$, and weak bands at 1478.0, 1670.6, 1714.3, 1777.9, 1792.6, and 1806.7 $cm^{-1}$. Annealing to 8 and 10 K increased the 1944.0, 1930.6, 1844.2, and 1478.0 $cm^{-1}$ bands, slightly decreased the weak bands at 1670.6, 1714.3, 1777.9, and 1806.7 $cm^{-1}$, and produced new bands at 1910.8, 1958.5, 1963.4, and 1984.3 $cm^{-1}$. A 15 min broad band photolysis destroyed the 1478.0, 1670.6, 1714.3, 1777.9, 1792.6, 1806.7, and 1930.6 $cm^{-1}$ absorptions. A final 12 K annealing recovered the 1478.0 and 1930.6 $cm^{-1}$ bands and increased the 1844.2, 1910.8, 1944.0, 1958.5, 1963.4, and 1984.3 $cm^{-1}$ bands.

Another experiment was done to explore the photochemistry more thoroughly, and spectra in the 1890−1660 $cm^{-1}$ region are shown in Figure 2. Annealing to 8 K decreased the 1670.6, 1714.3, and 1777.9 $cm^{-1}$ bands and produced weak 1835.1 and 1873.1 $cm^{-1}$ bands with little effect on other absorptions. Mercury arc photolysis using the 470 nm long-wavelength pass filter increased the 1714.3, 1792.6, 1835.1, and 1873.1 $cm^{-1}$ bands at the expense of the 1670.6, 1777.9, and 1806.7 $cm^{-1}$ bands. Photolysis using $\lambda > 380$ nm destroyed the 1670.6, 1777.9, and 1806.7 $cm^{-1}$ bands, while the 1714.3, 1792.6, 1835.1, and 1873.1 $cm^{-1}$ bands continued to increase. Additional photolysis with $\lambda > 290$ nm decreased the 1714.3 $cm^{-1}$ band and increased the 1835.1 and 1873.1 $cm^{-1}$ absorptions with no change for the 1792.6 $cm^{-1}$ band. A final full-arc photolysis eliminated the 1714.3, 1792.6, and 1835.1 $cm^{-1}$ bands and decreased the 1873.1 $cm^{-1}$ absorption.

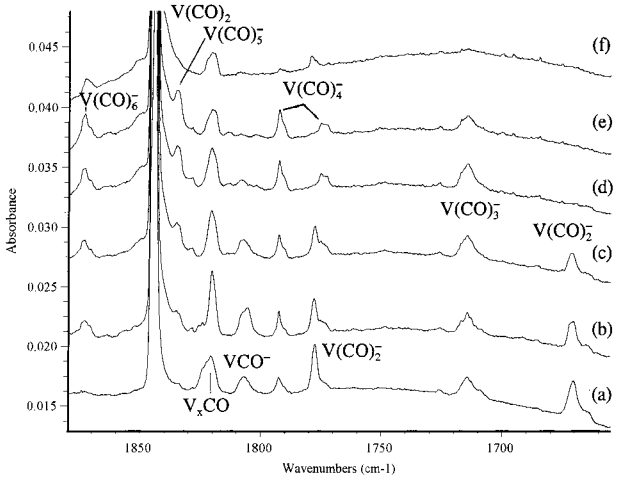


**Figure 2.** Infrared spectra in the 1880−1660 $cm^{-1}$ region from laser-ablated V atoms co-deposited with 0.1%CO in neon: (a) 30 min sample deposition at 4 K, (b) after annealing to 8 K, (c) after 15 min $\lambda > 470$ nm photolysis, (d) after 15 min $\lambda > 380$ nm photolysis, (e) after 15 min $\lambda > 290$ nm photolysis, and (f) after 15 min full arc photolysis.

Similar spectra were observed using isotopic $^{13}C^{16}O$ and $^{12}C^{18}O$ samples, and all of the new product absorptions exhibited isotopic shifts as listed in Table 1. The spectrum using a mixed $^{12}C^{16}O + {}^{13}C^{16}O$ sample is shown in Figure 3.

**Ti + CO/Ne.** Experiments were done using 0.1% and 0.05% CO in neon and lower laser power; Figure 4 shows the spectra in the 2070−1660 $cm^{-1}$ region with a 0.05% CO, and the absorptions are listed in Table 2. Spectra after deposition exhibited new absorptions at 1677.5, 1742.1, 1789.9, 1799.3, 1893.1, and 2041.3 $cm^{-1}$. Annealing to 6 K and 8 K increased the 2041.3 $cm^{-1}$ band and slightly decreased the other bands. Mercury arc photolysis using a $\lambda > 470$ nm almost destroyed the 1677.5, 1742.1, and 1789.9 $cm^{-1}$ bands and produced weak bands at 1730.9, 1760.6 1816.0, 1824.5, 1861.0, and 1920.0 $cm^{-1}$. Additional photolysis with $\lambda > 290$ nm eliminated the 1730.9, 1760.6, 1816.0, 1824.5, 1861.0, and 2041.3 $cm^{-1}$ bands.

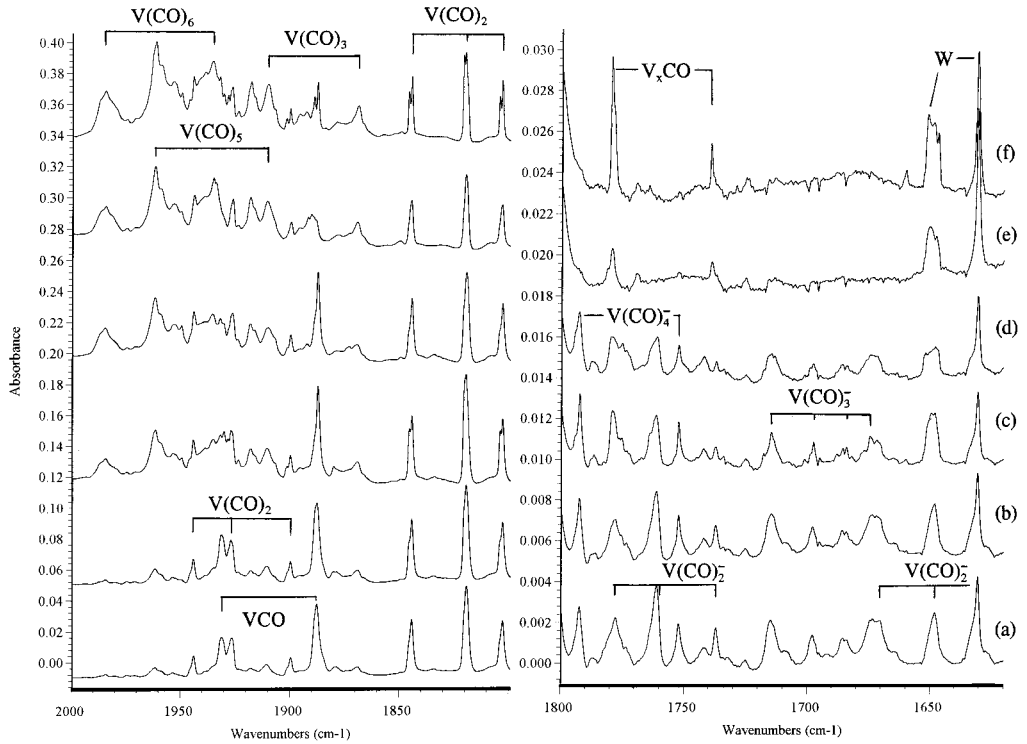


**Figure 3.** Infrared spectra in the 2000−1620 $cm^{-1}$ region from laser-ablated V atoms co-deposited with 0.1% $^{12}C^{16}O$ + 0.1% $^{13}C^{16}O$ in neon: (a) 45 min sample deposition at 4 K, (b) after annealing to 6 K, (c) after annealing to 9 K, (d) after 15 min $\lambda$ > 470 nm photolysis, (e) after 15 min full arc photolysis, and (f) after annealing to 11 K.

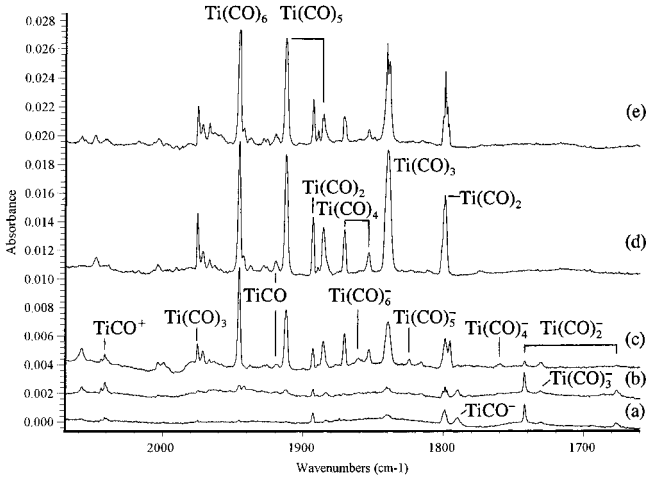


**Figure 4.** Infrared spectra in the 2070−1660 $cm^{-1}$ region from laser-ablated Ti atoms co-deposited with 0.05%CO in neon: (a) 30 min sample deposition at 4 K, (b) after annealing to 8 K, (c) after 15 min $\lambda$ > 470 nm photolysis, (d) after 15 min $\lambda$ >290 nm photolysis, and (e) after annealing to 10 K.

The 1799.3, 1840.3, 1853.5, 1871.0, 1885.7, 1912.5, 1920.0, 1945.7, and 1975.1 $cm^{-1}$ bands markedly increased on photolysis. Another experiment using 0.1% CO exhibited similar results and spectra in the 1870−1660 $cm^{-1}$ region, which contain anion absorptions, are shown in Figure 5. The 1677.5, 1730.9, 1742.1, and 1789.9 $cm^{-1}$ bands slightly decreased on 6 K and 8 K annealing, while the 1816.0, 1824.5, and 1861.0 $cm^{-1}$ bands increased. Photolysis using $\lambda$ > 470 nm almost eliminated the 1677.5, 1742.1, and 1789.9 $cm^{-1}$ bands, and the 1730.9, 1760.6, 1816.0, 1824.5, and 1861.0 $cm^{-1}$ bands increased. Additional photolysis at $\lambda$ > 380 nm destroyed the 1730.9 $cm^{-1}$ band while the 1816.0, 1824.5, and 1861.0 $cm^{-1}$ absorptions still increased. Another photolysis using $\lambda$ > 290 nm destroyed the 1816.0, 1824.5, and 1861.0 $cm^{-1}$ bands.

Again, isotopic experiments were done with $^{13}C^{16}O$, $^{12}C^{18}O$, and $^{12}C^{16}O$ + $^{13}C^{16}O$ samples, the isotopic counterparts are listed in Table 2, and the mixed $^{12}C^{16}O$ + $^{13}C^{16}O$ spectra are shown in Figure 5.

**$CCl_4$ Doping.** Experiments were done for both V and Ti systems with 0.1% CO in neon and 0.02% $CCl_4$ added to serve as an electron trap.[18−20] Briefly, the absorptions assigned below to anions were almost eliminated from the spectra of the deposited samples and were not produced on annealing and photolysis, whereas absorptions to be identified as cations were enhanced on doping with $CCl_4$.

**Argon Matrix Experiments.** Complementary argon matrix experiments were done with low laser power to contrast the thermal V experiments.[2] The present spectra using more dilute 0.4% CO in argon showed weaker absorptions, none of the bands were attributed to $V_x(CO)_y$ clusters, and a new feature was visible at 2116.3 $cm^{-1}$, which increased on annealing to 25 K and decreased on photolysis. The major bands on deposition at 10 K were observed at 1904.7 and 1895.8 $cm^{-1}$.

Likewise low laser power experiments were done with Ti and CO (0.4%) in argon to contrast the earlier higher power investigations.[10] The present spectra were cleaner: no TiO nor $TiO_2$ absorption was observed on deposition and even after 25 K annealing, the 917 $cm^{-1}$ $TiO_2$ absorption only reached 0.0004 AU. Weak bands were observed on deposition at 1997.0, 1887.8, 1882.5, 1877.3, 1865.5, 1776.4, and 1769.6 $cm^{-1}$; no 1854 band was observed here. Annealing to 20 K decreased all bands but increased the 1769.6 $cm^{-1}$ feature, and annealing to 25 K continued this trend and produced 1867.0, 1897.7, 1933.5, 1964.8, and 1995 $cm^{-1}$ bands. Photolysis ($\lambda$ > 470 nm) accentuated this growth, particularly at 1769.6, 1867.0, 1933.5, and 1964.8 $cm^{-1}$. After full-arc photolysis, the 1933.5 $cm^{-1}$ band dominated the spectrum.

**Calculations.** DFT calculations were done to support infrared band identifications using the Gaussian 94 program.[25] The BP86

**TABLE 2: Infrared Absorptions ($cm^{-1}$) from Co-deposition of Laser-Ablated Ti with Carbon Monoxide in Excess Neon at 4 K**

| $^{12}C^{16}O$ | $^{13}C^{16}O$ | $^{12}C^{18}O$ | $^{12}C^{16}O + {}^{13}C^{16}O$ | ratio (12/13) | ratio (16/18) | assignment |
|---|---|---|---|---|---|---|
| 2140.8 | 2093.6 | 2089.7 | | 1.0225 | 1.0245 | CO |
| 2057.9 | 2010.9 | | | | | $(Ti(CO)_2^+)$ ? |
| 2041.3 | 1996.4 | 1993.1 | 2041.2, 1996.2 | 1.0225 | 1.0242 | $TiCO^+$ |
| 1975.1 | 1930.6 | 1930.3 | 1975.2, 1962.9, 1948.5, 1930.6 | 1.0230 | 1.0232 | $Ti(CO)_3$ |
| 1945.7 | 1903.3 | 1898.9 | | 1.0223 | 1.0246 | $Ti(CO)_6$ |
| 1920.0 | 1876.0 | 1874.6 | | 1.0235 | 1.0242 | TiCO |
| 1912.5 | 1870.7 | 1865.9 | | 1.0223 | 1.0250 | $Ti(CO)_5$ |
| 1893.1 | 1850.0 | 1850.3 | 1893.0, 1875.9, 1850.0 | 1.0233 | 1.0231 | $Ti(CO)_2$ |
| 1885.6 | 1844.2 | 1841.1 | | 1.0224 | 1.0242 | $Ti(CO)_5$ |
| 1871.0 | 1830.4 | 1825.9 | | 1.0222 | 1.0247 | $Ti(CO)_4$ |
| 1861.0 | 1820.2 | 1817.0 | | 1.0224 | 1.0242 | $Ti(CO)_6^-$ |
| 1853.5 | 1812.3 | 1810.7 | | 1.0227 | 1.0236 | $Ti(CO)_4$ |
| 1840.3 | 1800.7 | 1797.3 | 1840.2, 1823.3, 1811.1, 1800.0 | 1.0220 | 1.0239 | $Ti(CO)_3$ |
| 1824.5 | 1784.7 | 1781.5 | | 1.0223 | 1.0241 | $Ti(CO)_5^-$ |
| 1816.0 | 1775.3 | 1773.5 | | 1.0229 | 1.0240 | $Ti(CO)_5^-$ site |
| 1799.3 | 1758.6 | 1758.3 | 1799.3, 1774.2, 1758.6 | 1.0231 | 1.0233 | $Ti(CO)_2$ |
| 1789.9 | 1749.5 | 1749.7 | | 1.0231 | 1.0230 | $TiCO^-$ |
| 1781.8 | 1742.7 | 1741.1 | | 1.0224 | 1.0234 | $Ti_x(CO)_y^-$ |
| 1760.6 | 1721.0 | 1719.6 | | 1.0230 | 1.0238 | $Ti(CO)_4^-$ |
| 1742.1 | 1702.7 | 1702.3 | 1742.1, 1728.0, 1702.9 | 1.0231 | 1.0234 | $Ti(CO)_2^-$ |
| 1730.9 | 1692.6 | 1691.4 | | 1.0226 | 1.0231 | $Ti(CO)_3^-$ |
| 1677.5 | 1638.9 | 1639.7 | 1677.0, 1651.3, 1638.9 | 1.0236 | 1.0231 | $Ti(CO)_2^-$ |
| 1517.4 | 1484.2 | 1481.2 | 1517.4, 1499.4, 1484.2 | 1.0224 | 1.0244 | $(CO)_2^-$ |
| 1516.3 | 1483.0 | 1480.4 | 1516.3, 1498.1, 1483.0 | 1.0225 | 1.0243 | $(CO)_2^-$ site |

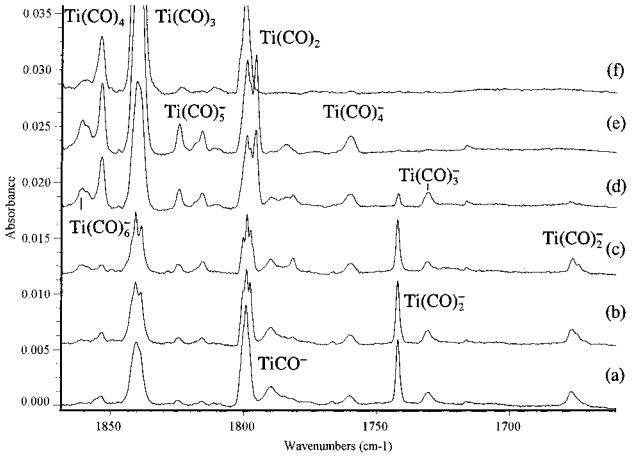


**Figure 5.** Infrared spectra in the 1870−1660 $cm^{-1}$ region from laser-ablated Ti atoms co-deposited with 0.1%CO in neon: (a) 30 min sample deposition at 4 K, (b) after annealing to 6 K, (c) after annealing to 8 K, (d) after 15 min $\lambda > 470$ nm photolysis, (e) after 15 min $\lambda > 380$ nm photolysis, and (f) after 15 min $\lambda > 290$ nm photolysis.

and B3LYP functionals, 6-311 + G* basis sets for C and O atoms, and the all-electron set of Wachters and Hay as modified by Gaussian 94 for vanadium and titanium atoms were used to calculate structures and frequencies.[26−28] Adamo and Lelj investigated CO and FeCO with both BP86 and B3LYP functionals and found that the calculated BP86 frequencies were lower and closer to observed values than are B3LYP frequencies.[16] Calculations were performed on the monocarbonyl neutrals, cations, and anions, and the results are listed in Table 3 for both functionals. In agreement with previous calculations,[13,15,16] the VCO molecule has a $^6\Sigma^+$ ground state and TiCO has a $^5\Delta$ ground state, which correlate with metastable excited metal atoms $3d^44s^1(^6D)$ V and $3d^34s^1(^5F)$ Ti and ground state ($^1\Sigma^+$) CO. The lower spin state carbonyls, which correlate with ground-state metal atoms, are 8.8 and 14.4 kcal/mol *higher*, respectively. Both $VCO^+$ and $VCO^-$ were calculated to have $^5\Sigma^+$ ground states, whereas $TiCO^+$ and $TiCO^-$ were calculated to have $^4\Delta$ ground states. A previous investigation also found $^5\Sigma^+$ and $^4\Delta$ ground states for the $VCO^+$ and $TiCO^+$ cations.[14]

It will be shown below that BP86 frequencies are closer to the observed frequencies than are B3LYP values for TiCO and VCO species. Accordingly, BP86 calculations were done for dicarbonyl species, and the results are listed in Table 4. Previous ab initio calculations on $Ti(CO)_2$ and $V(CO)_2$ molecules favor the linear geometry,[13] but our infrared spectra show that these species have bent structures, so only bent geometries were considered. For $V(CO)_2$, two states, namely $^4B_2$ and $^6A_1$, are very close in energy, with the $^4B_1$ state about 1.2 kcal/mol lower. For the $V(CO)_2^-$ anion, the $^5A_1$ state was calculated to be only 0.5 kcal/mol lower than the $^7A_1$ state. The same trend was found for $Ti(CO)_2$: our calculation predicted a $^3B_2$ state 4.6 kcal/mol lower than the $^5A_1$ state, whereas a $^4B_2$ state is 6.2 kcal/mol lower in energy than the $^6A_1$ state for the $Ti(CO)_2^-$ anion. Table 4 shows that the higher spin states have longer M−C bonds, shorter C−O bonds, and more open C−M−C angles for both neutrals and anions. The $V(CO)_2^+$ and $Ti(CO)_2^+$ cations were calculated to have $^5B_2$ and $^4B_2$ ground states with bent geometries, but previous calculations only considered linear structures.[14]

Finally, calculations were done for tricarbonyls and their anions, and the results are listed in Table 5. The $V(CO)_3$ molecule was calculated to have a $^2A_1$ ground state with $C_{3v}$ symmetry, but a $^6A_1$ state with $C_{3v}$ symmetry is only 4.4 kcal/mol higher. The $V(CO)_3^-$ anion also has a $^1A_1$ ground state with $C_{3v}$ symmetry. The $Ti(CO)_3$ molecule was calculated to have a $^3A_1$ ground state with $C_{3v}$ symmetry, while the $Ti(CO)_3^-$ anion has a $^2A'$ ground state with $C_{2v}$ symmetry, but a $^4A_1$ state with $C_{3v}$ geometry is 7.2 kcal/mol higher in energy.

## Discussion

Infrared absorption bands are assigned to titanium and vanadium carbonyl neutral, anion, and cation species on the basis of annealing and photolysis behavior, isotopic substitution, and DFT isotopic frequency calculations. One problem is how accurately to expect the present BP86 functional and basis set to match the observed frequencies for the open-shell TiCO and VCO molecules and related species.

**V(CO)*x* (*x* = 1−6).** The prominent absorption at 1930.6 $cm^{-1}$ observed on deposition increased on annealing to 8 and

**TABLE 3: Geometries, Relative Energy (kcal/mol), Harmonic Frequencies ($cm^{-1}$), and Intensities (km/mol) Calculated for VCO, $VCO^-$, $VCO^+$ and TiCO, $TiCO^-$, $TiCO^+$ with BP86 and B3LYP Functionals**

| | molecule | relative energy | geometry | $^{12}C^{16}O$ | $^{13}C^{16}O$ | $^{12}C^{18}O$ |
|---|---|---|---|---|---|---|
| BP86 | VCO | 0 | V−C: 1.967 Å | 1925.7 (1021) | 1881.3 (968) | 1881.6 (984) |
| | ($^6\Sigma^+$) | | C−O: 1.168 Å | 440.2 (10) | 435.6 (10) | 430.0 (9) |
| | | | linear | 279.0 (3) | 270.7(2) | 275.5 (3) |
| | VCO | +15.1 | V−C: 1.868 Å | 1845.0 (846) | 1801.8 (803) | 1803.8 (813) |
| | ($^4\Phi$) | | C−O: 1.184 Å | 498.1 (3) | 493.1 (3) | 486.4 (2) |
| | | | linear | 336.4 (19) | 326.3(17) | 332.3 (19) |
| | $VCO^-$ | −17.4 | V−C: 1.960 Å | 1819.7 (1119) | 1776.9 (1069) | 1779.1 (1067) |
| | ($^5\Sigma^+$) | | C−O: 1.186 Å | 448.9 (2) | 444.4 (3) | 438.3 (2) |
| | | | linear | 270.9(36) | 262.9(35) | 267.6 (36) |
| | $VCO^-$ | −14.8 | V−C: 1.996 Å | 1783.3 (1057) | 1741.3 (1027) | 1743.7 (984) |
| | ($^7\Sigma^+$) | | C−O: 1.193 Å | 419.7 (41) | 415.5 (38) | 409.7 (38) |
| | | | linear | 238.3 (29) | 231.2 (28) | 235.3 (29) |
| | $VCO^+$ | +161.3 | V−C: 2.046 Å | 2098.5 (389) | 2051.0 (367) | 2049.0 (378) |
| | ($^5\Sigma^+$) | | C−O: 1.141 Å | 370.0 (2) | 366.0 (2) | 361.7 (1) |
| | | | linear | 275.3 (2) | 267.3 (2) | 271.7 (2) |
| | | | | 273.2 (2) | 265.2 (2) | 269.7 (2) |
| | TiCO | 0 | Ti−C: 2.015 Å | 1887.9 (991) | 1844.7 (939) | 1844.1 (956) |
| | ($^5\Delta$) | | C−O: 1.174 Å | 424.8 (12) | 420.3 (12) | 415.3 (11) |
| | | | linear | 276.1 (1) | 268.0 (1) | 272.6 (2) |
| | $TiCO^-$ | −21.1 | Ti−C: 2.009 Å | 1779.8 (1128) | 1738.5 (1058) | 1739.5 (1056) |
| | ($^4\Delta$) | | C−O: 1.192 Å | 434.4 (4) | 430.0 (4) | 424.5 (4) |
| | | | linear | 276.6 (17) | 268.5 (16) | 273.2 (17) |
| | $TiCO^+$ | +152.9 | Ti−C: 2.064 Å | 2035.4 (434) | 1989.4 (410) | 1987.4 (421) |
| | ($^4\Delta$) | | C−O: 1.150 Å | 390.0 (1) | 385.8 (1) | 381.5 (1) |
| | | | linear | 281.8 (7) | 273.5 (7) | 278.1 (7) |
| B3LYP | VCO | 0 | V−C: 1.996 Å | 2004.5 (1815) | 1959.4 (1713) | 1956.8 (1761) |
| | ($^6\Sigma^+$) | | C−O: 1.150 Å | 401.9 (63) | 397.5 (63) | 393.0 (59) |
| | | | linear | 260.3 (0.1) | 252.7 (0.1) | 257.0 (0.1) |
| | VCO | +13.5 | V−C: 1.916 Å | 1926.2 (1253) | 1881.6 (1193) | 1882.3 (1202) |
| | ($^4\Phi$) | | C−O: 1.168 Å | 443.1 (2) | 438.5 (2) | 432.8 (2) |
| | | | linear | 323.2 (11) | 313.7 (10) | 319.2 (12 |
| | | | | 305.0 (2) | 296.0 (1) | 301.3 (2) |
| | $VCO^-$ | −15.8 | V−C: 1.968 Å | 1855.1 (1921) | 1812.4 (1829) | 1812.5 (1840) |
| | ($^5\Sigma^+$) | | C−O: 1.172 Å | 443.0 (16) | 438.3 (17) | 432.8 (16) |
| | | | linear | 271.7 (34) | 263.7 (32) | 268.3 (33) |
| | $VCO^-$ | −10.0 | V−C: 1.992 Å | 1819.2 (1464) | 1776.5 (1419) | 1778.6 (1366) |
| | ($^7\Sigma^+$) | | C−O: 1.184 Å | 430.4 (48) | 426.1 (45) | 420.3 (45) |
| | | | linear | 254.5 (23) | 247.0 (22) | 251.3 (22) |
| | $VCO^+$ | +149.4 | V−C: 2.121 Å | 2215.7 (394) | 2165.9 (371) | 2162.8 (384) |
| | ($^5\Sigma^+$) | | C−O: 1.125 Å | 323.1 (4) | 319.5 (4) | 316.0 (4) |
| | | | linear | 264.9 (1) | 257.2 (1) | 261.3 (1) |
| | TiCO | 0 | Ti−C: 2.042 Å | 1972.3 (1424) | 1927.9 (1346) | 1925.4 (1378) |
| | ($^5\Delta$) | | C−O: 1.156 Å | 398.9 (38) | 394.6 (37) | 390.2 (35) |
| | | | linear | 263.4 (0.1) | 255.7 (0.1) | 260.0 (0.1) |
| | $TiCO^-$ | −19.8 | Ti−C: 2.019 Å | 1834.9 (1634) | 1793.0 (1556) | 1792.2 (1566) |
| | ($^4\Delta$) | | C−O: 1.177 Å | 426.4 (19) | 421.9 (20) | 416.9 (18) |
| | | | linear | 269.6 (21) | 261.7 (20) | 266.2 (20) |
| | $TiCO^+$ | +144.8 | Ti−C: 2.120 Å | 2155.7 (564) | 2107.4 (530) | 2104.1 (549) |
| | ($^4\Delta$) | | C−O: 1.132 Å | 349.9 (6) | 346.1 (5) | 342.4 (5) |
| | | | linear | 273.7 (5) | 265.7 (4) | 270.0 (5) |

10 K, but decreased on photolysis. This band shifted to 1887.5 $cm^{-1}$ in $^{13}C^{16}O$ and to 1885.8 $cm^{-1}$ in $^{12}C^{18}O$ experiments giving the 12/13 and 16/18 ratios 1.0228 and 1.0238, respectively, which are near the diatomic CO values. In the mixed $^{12}C^{16}O + {}^{13}C^{16}O$ experiment, only pure isotopic counterparts were observed, indicating that only one CO subunit is involved in this mode. The 1930.6 $cm^{-1}$ band is assigned to the VCO molecule, which is in good agreement with the 1904 $cm^{-1}$ argon matrix value.[2] Our DFT calculations predicted the C−O stretching vibration at 1925.7 $cm^{-1}$ (BP86) and 2004.5 $cm^{-1}$ (B3LYP) for ground state ($^6\Sigma^+$) VCO, which correlates with $^6$D metastable atomic V. Recall that $^6$D vanadium is 0.26 eV above the ground $^4$F state. As will be discussed below, we believe that the V + CO reaction is assisted by electronic excitation from the infrared source.

The sharp strong bands at 1844.2 and 1944.0 $cm^{-1}$ exhibit the same profile and increase together on annealing, suggesting that they are due to different modes of the same molecule. Both bands showed carbonyl C−O stretching frequency ratios, and the upper band has slightly more C and less O participation than the lower band. In the mixed $^{12}C^{16}O + {}^{13}C^{16}O$ experiment, triplets with 1/2/1 intensity distribution were observed for both bands, which are appropriate for antisymmetric and symmetric vibrational modes of a bent $V(CO)_2$ molecule. Matching asymmetries in these triplets, i.e., displacement of the central $(O^{12}C)V(^{13}CO)$ components in each band system due to interaction, further associates these bands. Our BP86 calculation strongly supports these assignments: the antisymmetric and symmetric vibrations of $^4B_2$ ground-state $V(CO)_2$ are predicted at 1859.5 and 1925.9 $cm^{-1}$. Of more importance, the calculated isotopic ratios (12/13: 1.0237, 1.0239. 16/18: 1.0231, 1.0234) are in good agreement with the observed values listed in Table 1.

Our assignment is in accord with the matrix ESR study, which suggested a bent quartet state,[4] but in disagreement with previous IR assignments in Ar, Kr, and Xe matrixes, where three forms of $V(CO)_2$ were inferred.[2] We suggest that the 1723, 1719 $cm^{-1}$ argon matrix band is too low for a terminal dicarbonyl C−O

**TABLE 4: Geometries, Relative Energy (kcal/mol), C−O Stretching Vibrational Frequencies (cm$^{-1}$), and Intensities (km/mol) Calculated (BP86/6-311+G*) for V(CO)$_2$, V(CO)$_2^+$, V(CO)$_2^-$ and Ti(CO)$_2$, Ti(CO)$_2^+$, Ti(CO)$_2^-$**

| molecule | relative energy | geometry | $(12-16)_2$ | $(13-16)_2$ | $(12-18)_2$ |
|---|---|---|---|---|---|
| $V(CO)_2$ | 0 | V−C: 1.904 Å | 1925.9 (625) | 1881.0 (593) | 1882.5 (601) |
| ($^4B_2$) | | C−O: 1.173 Å | 1859.5 (1215) | 1816.5 (1151) | 1817.0 (1173) |
| | | ∠CVC: 86.9° | | | |
| | | ∠VCO: 178.5° | | | |
| $V(CO)_2$ | +1.2 | V−C: 2.014 Å | 1965.4 (309) | 1920.0 (294) | 1920.4 (296) |
| ($^6A_1$) | | C−O: 1.165 Å | 1920.0 (1848) | 1876.3 (1752) | 1875.1 (1782) |
| | | ∠CVC: 130° | | | |
| | | ∠VCO: 170.1° | | | |
| $V(CO)_2^-$ | −22.4 | V−C: 1.917 Å | 1777.0 (1354) | 1735.3 (1291) | 1737.3 (1295) |
| ($^5A_1$) | | C−O: 1.197 Å | 1719.2 (990) | 1678.9 (928) | 1680.9 (971) |
| | | ∠CVC: 100.4° | | | |
| | | ∠VCO: 173.9° | | | |
| $V(CO)_2^-$ | −21.9 | V−C: 2.015 Å | 1813.5 (689) | 1771.1 (661) | 1772.7 (653) |
| ($^7A_1$) | | C−O: 1.188 Å | 1792.7 (1543) | 1750.9 (1482) | 1752.2 (1458) |
| | | ∠CVC: 134.7° | | | |
| | | ∠VCO: 177.7° | | | |
| $V(CO)_2^+$ | +162.1 | V−C: 2.047 Å | 2110.8 (201) | 2062.9 (189) | 2061.1 (195) |
| ($^5B_2$) | | C−O: 1.141 Å | 2075.6 (671) | 2028.9 (631) | 2026.2 (653) |
| | | ∠CVC: 91.6° | | | |
| | | ∠VCO: 178.9° | | | |
| $Ti(CO)_2$ | 0 | Ti−C: 1.961 Å | 1862.0 (944) | 1819.3 (895) | 1819.0 (911) |
| ($^3B_2$) | | C−O: 1.180 Å | 1817.5 (1068) | 1775.5 (1014) | 1775.9 (1026) |
| | | ∠CTiC: 81.2° | | | |
| | | ∠TiCO: 178.1° | | | |
| $Ti(CO)_2$ | +4.6 | Ti−C: 2.076 Å | 1918.4 (453) | 1874.4 (429) | 1874.2 (435) |
| ($^5A_1$) | | C−O: 1.169 Å | 1875.4 (2717) | 1833.3 (2572) | 1830.6 (2625) |
| | | ∠CTiC: 139.0° | | | |
| | | ∠TiCO: 171.7° | | | |
| $Ti(CO)_2^-$ | −34.7 | Ti−C: 1.971 Å | 1762.4 (1716) | 1721.6 (1636) | 1722.3 (1642) |
| ($^4B_2$) | | C−O: 1.197 Å | 1718.3 (1022) | 1678.2 (974) | 1679.8 (978) |
| | | ∠CTiC: 82.6° | | | |
| | | ∠TiCO: 177.9° | | | |
| $Ti(CO)_2^-$ | −28.1 | Ti−C: 2.039 Å | 1775.3 (971) | 1734.1 (927) | 1734.9 (926) |
| ($^6A_1$) | | C−O: 1.194 Å | 1754.9 (1307) | 1714.1 (1257) | 1715.2 (1236) |
| | | ∠CTiC: 120.6° | | | |
| | | ∠TiCO: 172.0° | | | |
| $Ti(CO)_2^+$ | +149.3 | Ti−C: 2.082 Å | 2072.2 (209) | 2025.3 (197) | 2023.4 (202) |
| ($^4B_2$) | | C−O: 1.147° | 2024.4 (859) | 1979.1 (810) | 1975.9 (834) |
| | | ∠CTiC: 90.4° | | | |
| | | ∠TiCO: 178.6° | | | |

**TABLE 5: Geometries, Relative Energy (kcal/mol), C−O Stretching Vibrational Frequencies (cm$^{-1}$), and Intensities (Km/mol) Calculated (BP86/6-311+G*) for V(CO)$_3$, V(CO)$_3^-$ and Ti(CO)$_3$, Ti(CO)$_3^-$**

| molecule | relative energy | $(12-16)_3$ | $(13-16)_3$ | $(12-18)_3$ |
|---|---|---|---|---|
| $V(CO)_3$ | 0 | 1957.6 (158) ($a_1$) | 1911.8 (150) | 1913.8 (152) |
| ($^2A_1$)[a] | | 1799.5 (2095) (e) | 1760.7 (1970) | 1754.4 (2040) |
| $V(CO)_3$ | +4.4 | 2004.1 (50) | 1958.0 (47) | 1957.9 (48) |
| ($^6A_1$)[b] | | 1940.8 (1611) | 1896.8 (1528) | 1895.2 (1552) |
| $V(CO)_3^-$ | −50.4 | 1796.2 (789) ($a_1$) | 1753.2 (750) | 1757.6 (759) |
| ($^1A_1$)[c] | | 1707.9 (1368) (e) | 1667.1 (1303) | 1670.9 (1310) |
| $Ti(CO)_3$ | 0 | 1947.8 (363) ($a_1$) | 1902.8 (346) | 1903.3 (348) |
| ($^3A_1$)[d] | | 1855.8 (1169) (e) | 1813.7 (1108) | 1812.1 (1128) |
| $Ti(CO)_3^-$ | −36.2 | 1792.7 (2724) | 1751.0 (2585) | 1752.2 (2624) |
| ($^2A'$)[e] | | 1725.5 (685) | 1684.9 (653) | 1687.3 (655) |
| | | 1725.3 (1554) | 1685.8 (1554) | 1685.5 (1568) |
| $Ti(CO)_3^-$ | −29.0 | 1879.4 (843) ($a_1$) | 1835.7 (812) | 1836.9 (793) |
| ($^4A_1$)[f] | | 1776.9 (756) (e) | 1736.5 (715) | 1735.5 (726) |

[a] Structure: $C_{3v}$ symmetry, V−C: 1.899 Å, C−O: 1.172 Å, ∠CVC: 95.4°, ∠VCO: 179.7°. [b] Structure: $C_{3v}$ symmetry, V−C: 2.038 Å, C−O: 1.160 Å, ∠CVC: 117.4°, ∠VCO: 175.6°. [c] Structure: $C_{3v}$ symmetry, V−C: 1.843 Å, C−O: 1.202 Å, ∠CVC: 87.3°, ∠VCO: 179.7°. [d] Structure: $C_{3v}$ symmetry, Ti−C: 1.994 Å, C−O: 1.171 Å, ∠CTiC: 82.4°, ∠TiCO: 178.9°. [e] Structure: $C_s$ symmetry, axial Ti−C: 1.942 Å, C−O: 1.197 Å, ∠TiCO: 178.8°, equatorial Ti−C: 1.969 Å, C−O: 1.194 Å, ∠CTiC: 100.5°, ∠TiCO: 176.1°, ∠CaxTiCeq: 73.9°. [f] Structure: $C_{3v}$ symmetry, Ti−C: 2.012 Å, C−O: 1.183 Å, ∠CTiC: 81.0°, ∠TiCO: 178.9°.

stretching vibration, and most likely is due to a bridged dimetal dicarbonyl species, whereas the higher 1974, 1982 cm$^{-1}$ band is probably due to a metal cluster species. However, the 1820 cm$^{-1}$ band is probably due to V(CO)$_2$ as counterpart to the present 1844.2 cm$^{-1}$ neon matrix band. In the gas-phase time-resolved infrared study,[5] the 2025 cm$^{-1}$ absorption tentatively assigned to V(CO)$_2$ is also too high and probably is due to another cluster species.

There is disagreement on V(CO)$_3$ between matrix and gas-phase infrared reports.[2,4,5] An argon matrix 1920 cm$^{-1}$ band was assigned to the trigonal species, whereas a gas phase 1859 cm$^{-1}$ absorption was identified with V(CO)$_3$. Our DFT calculation predicted a $^2A_1$ ground state with $C_{3v}$ geometry, and a strong doubly degenerate C−O vibration at 1799.5 cm$^{-1}$ for V(CO)$_3$; however, a $^6A_1$ state is only 4.4 kcal/mol higher with a strong doubly degenerate C−O vibration at 1940.8 cm$^{-1}$. In our spectra, no obvious band in the 1900−1800 cm$^{-1}$ region can be assigned to this molecule. A 1910.8 cm$^{-1}$ band increases on annealing after V(CO)$_2$ and before the next carbonyl species and gives the isotopic ratios (12/13: 1.0224, 16/18: 1.0251), but no obvious intermediate component was observed in the mixed $^{12}C^{16}O + {}^{13}C^{16}O$ experiment, which is appropriate for V(CO)$_3$.

The V(CO)$_4$ molecule was associated with bands at 1893 cm$^{-1}$ in an argon matrix[2] and at 1920 cm$^{-1}$ in the gas phase,[5] but both of these are likely to be incorrect. Our best candidate is at 1949.3 cm$^{-1}$, but this is a tentative suggestion.

The 1963.4 and 1958.5 cm$^{-1}$ absorptions increase together on annealing and are assigned to V(CO)$_5$, which is in good agreement with 1965 cm$^{-1}$ gas-phase value[5] and 1952, 1943 cm$^{-1}$ argon matrix absorptions.[2] The 1984.3 cm$^{-1}$ neon matrix band, which grows more and dominates on higher temperature annealing, is assigned to V(CO)$_6$ according to the 1988 cm$^{-1}$

gas phase and 1976 $cm^{-1}$ argon matrix values for the $V(CO)_6$ compound.[2,29]

**$V(CO)_x^-$ ($x = 1-6$).** At lower frequency in the 1830−1670 $cm^{-1}$ region, weak new photosensitive bands were observed. These bands share the common behavior of reduction to <10% of former yield on $CCl_4$ doping. The weak band at 1806.7 $cm^{-1}$ decreased on $\lambda > 470$ nm photolysis and disappeared on $\lambda > 380$ nm photolysis. The $^{13}C^{16}O$ and $^{12}C^{18}O$ counterparts at 1764.7 and 1766.3 $cm^{-1}$ gave isotopic ratios (12/13: 1.0238, 16/18: 1.0228), which are characteristic of small carbonyl C−O stretching modes. The photolysis and $CCl_4$ doping behavior indicate the anion assignment. Our DFT calculations predict $^5\Sigma^+$ ground-state $VCO^-$ anion with a C−O stretching vibration at 1819.7 $cm^{-1}$ (BP86) and 1855.1 $cm^{-1}$ (B3LYP). Note that the calculated ratios [(BP86) 12/13: 1.0241, 16/18: 1.0228, (B3LYP) 12/13: 1.0236, 16/18: 1.0235] are in excellent agreement (BP86 fits better) with observed values, which confirms the $VCO^-$ assignment. Also note that our BP86 frequency calculation is 4.9 $cm^{-1}$ low for VCO and 13.0 $cm^{-1}$ high for $VCO^-$, but the B3LYP values are 73.9 $cm^{-1}$ high for VCO and 48.4 $cm^{-1}$ high for $VCO^-$.

Sharp bands at 1670.6 and 1777.9 $cm^{-1}$ decreased together on annealing and photolysis. Both bands exhibited carbonyl isotopic ratios. In the mixed $^{12}C^{16}O + {}^{13}C^{16}O$ experiment, a 1/2/1 triplet was observed for the upper band, and the mixed isotopic counterpart of the lower band was covered by impurity water absorption. These two bands are assigned to symmetric and antisymmetric C−O stretching vibrations of the bent $V(CO)_2^-$ anion. The $V(CO)_2^-$ anion assignments are confirmed by DFT calculations. The BP86 calculation gave a $^5A_1$ ground state for the bent $V(CO)_2^-$ anion with antisymmetric and symmetric stretching frequencies at 1719.2 and 1777.0 $cm^{-1}$. The calculated intensity of the symmetric stretching vibration is higher than for the antisymmetric stretching modes, which is in accord with observed intensity distributions. Of more importance, the calculated 12/13 and 16/18 isotopic ratios for two stretching modes (1.0240, 1.0228 and 1.0240, 1.0229, respectively) are in excellent agreement with the observed values (1.0236, 1.0228 and 1.0234, 1.0228, respectively).

The broad 1714.3 $cm^{-1}$ band slightly decreased on annealing and slightly *increased* on photolysis with 470 and 380 nm long-wavelength pass filters, when the $VCO^-$ and $V(CO)_2^-$ absorptions decreased (Figure 2(d)). In the mixed $^{12}C^{16}O + {}^{13}C^{16}O$ experiment, a quartet with two weaker intermediate components was observed, which is characteristic of the doubly degenerate mode of a trigonal $M(CO)_3$ species.[30] This band is assigned to antisymmetric C−O vibration of the $V(CO)_3^-$ anion. Our DFT calculation predicted the $V(CO)_3^-$ anion to have a $^1A_1$ ground state with $C_{3v}$ geometry; the antisymmetric and symmetric vibrations were calculated at 1707.9 and 1796.2 $cm^{-1}$ with intensity distributions of 1368 × 2 to 789. The symmetric vibration is probably too weak to be observed or is overlapped by other absorptions.

The 1792.6 $cm^{-1}$ band slightly increased on 8 K annealing and photolysis using 470 and 380 nm long-wavelength pass filters, along with the $V(CO)_3^-$ absorption, but continued to increase with $\lambda > 290$ nm photolysis which decreased $V(CO)_3^-$. The 1792.6 $cm^{-1}$ band was almost destroyed by full-arc photolysis. A weak band at 1775.3 $cm^{-1}$, which is about 30% of the 1792.6 $cm^{-1}$ band intensity, has the same photolysis behavior. These two bands are most probably due to the $V(CO)_4^-$ anion with $C_{2v}$ symmetry (as is the isoelectronic $Cr(CO)_4$ molecule).[31] Extended Huckel calculations[11] suggest that $V(CO)_4^-$ is a singlet or triplet state. Because the $V(CO)_4^-$ absorption increased on annealing, the singlet ground state is preferred for a reaction product of singlet $V(CO)_3^-$.

The weak 1835.1 $cm^{-1}$ band produced on annealing increased on $\lambda > 290$ nm photolysis but disappeared on full-arc photolysis, which is suitable for $V(CO)_5^-$. Molecular orbital calculations suggest that the $V(CO)_5^-$ is a $C_{4v}$ singlet.[11,12] Buckner and coworkers suggest that $V(CO)_5^-$ is a triplet from the observation of low reactivity with two-electron donor ligands in the gas phase.[32] Our experiments suggest that $V(CO)_5^-$ has a singlet ground state as it is produced on annealing from CO addition to $V(CO)_4^-$.

The weak 1873.1 $cm^{-1}$ band produced on annealing and increased on $\lambda > 290$ nm photolysis was decreased only 50% by full arc photolysis. This band is assigned to $V(CO)_6^-$, which is in good agreement with 1864 $cm^{-1}$ argon matrix value.[6]

The selective photolysis behavior shows that more energetic radiation is required for destruction of anions containing more CO submolecules, which is in accord with recently reported Fe, Co, and Ni carbonyl anion photochemistry.[18−20] The absorptions assigned to $V(CO)_x^-$ anions were almost eliminated in the $CCl_4$ doping experiment, which adds further support for the anion identifications. Furthermore, the annealing behaviors of $V(CO)_x$ and $V(CO)_x^-$ ($x = 1-6$) are parallel.

**$Ti(CO)_x$ ($x = 1-6$).** The TiCO molecule has a $^5\Delta$ ground state, which correlates with $^5F$ excited-state Ti lying 0.78 eV higher than the $^3F$ ground-state atom,[13−16] and a C−O stretching vibration calculated at 1887.9 $cm^{-1}$ (BP86) and 1972.3 $cm^{-1}$ (B3LYP). This suggests that ground-state Ti atoms cannot react with CO to form TiCO. In present neon matrix experiments, a very weak band at 1920.0 $cm^{-1}$ greatly increased on photolysis particularly in the UV region. The observed isotopic 12/13 and 16/18 ratios (1.0235, 1.0242) are very close to the ratios calculated for TiCO [(BP86) 1.0234, 1.0238; (B3LYP) 1.0230, 1.0244], which strongly supports the TiCO assignment. Note that this band is slightly enhanced by $CCl_4$ doping when the $TiCO^-$ anion is eliminated owing to electron capture by $CCl_4$. The same growth on photolysis and enhancement with added $CCl_4$ was found for ScCO, where the same BP86 calculation was 10 $cm^{-1}$ lower than the observed neon matrix value.[33]

The sharp 1887.8 $cm^{-1}$ argon matrix band behaves just as the 1920.0 $cm^{-1}$ neon matrix band in the present low laser energy experiments; it decreases slightly on 20, 25 K annealing, and increases slightly with $\lambda > 470$ nm, $\lambda > 380$ nm, and full-arc photolysis. This is one of two bands considered for TiCO in the earlier argon matrix study,[10] but another 1854.4 $cm^{-1}$ band, not observed here, was assigned to TiCO. The sharp 1887.8 $cm^{-1}$ band is here reassigned to TiCO in solid argon. The 32.2 $cm^{-1}$ argon-to-neon blue shift demonstrates a considerable matrix interaction for TiCO.

Sharp bands at 1799.3 and 1893.1 $cm^{-1}$ are the major product absorptions after deposition, which decreased together on annealing and increased on photolysis. Both bands produced triplets with 1/2/1 intensity distribution in mixed experiment, and are assigned to antisymmetric and symmetric C−O stretching vibrations of the bent $Ti(CO)_2$ molecule. Again, matching asymmetries in the triplets (separations 15.6 and 25.1 $cm^{-1}$ in the lower band with 25.9 and 17.1 $cm^{-1}$ in the upper band, respectively) show that these two bands belong to the same molecule. DFT calculation predicted a $^3B_2$ state and a $^5A_1$ state close in energy, with the $^3B_2$ state slightly lower. The calculated vibrational frequencies (1817.5, 1862.0 $cm^{-1}$) and isotopic ratios (12/13: 1.0237, 1.0235, 16:18: 1.0234, 1.0236) of the $^3B_2$ state fit the experimental values quite well.

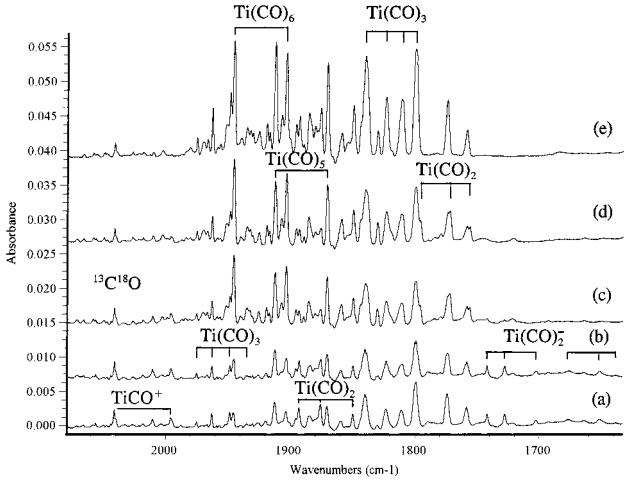


**Figure 6.** Infrared spectra in the 2080−1630 $cm^{-1}$ region from laser-ablated Ti atoms co-deposited with 0.1% $^{12}C^{16}O$ + 0.1% $^{13}C^{16}O$ in neon: (a) 45 min sample deposition at 4 K, (b) after annealing to 6 K, (c) after 15 min $\lambda > 470$ nm photolysis, (d) after 15 min $\lambda > 380$ nm photolysis, and (f) after 15 min $\lambda > 290$ nm photolysis.

The 1840.3 $cm^{-1}$ band decreased on annealing, increased markedly on photolysis, and exhibited carbonyl stretching vibrational ratios as does the associated weaker 1975.1 $cm^{-1}$ band, which maintained constant relative intensity. The mixed $^{12}C^{16}O$ + $^{13}C^{16}O$ spectra shown in Figure 6 demonstrates that these two bands are due to a trigonal molecule with $C_{3v}$ symmetry. The approximately 2:1:1:2 relative intensities of the lower band are characteristic of a doubly degenerate antisymmetric C−O stretching mode for a trigonal species.[30] The approximately 1:3:3:1 relative intensities for the upper band, on the other hand, are characteristic of the nondegenerate symmetric C−O stretching mode for three equivalent CO submolecules. The assignments are strongly supported by DFT calculations as listed in Table 5. Note that the calculation predicted a strong antisymmetric C−O stretching vibration at 1855.8 $cm^{-1}$ (1169 × 2 km/mol) and a much weaker symmetric vibration at 1947.8 $cm^{-1}$ (363 km/mol). The calculated isotopic frequency ratios are also in good agreement with the observed values, which show a slight change in carbon participation in the two different modes.

There are several major product absorptions at 1853.5, 1871.0, 1885.6, 1912.5, and 1945.7 $cm^{-1}$, which increased greatly on photolysis. All of these bands exhibited carbonyl C−O stretching vibrational ratios. The 1853.5 $cm^{-1}$ band tracks with the 1871.0 $cm^{-1}$ band; both are probably due to the $Ti(CO)_4$ molecule with $C_{2v}$ symmetry like the $Cr(CO)_4$ and $Fe(CO)_4$ molecules.[31,34] There are no obvious intermediates for the 1885.6, 1912.5, and 1945.7 $cm^{-1}$ bands in the mixed $^{12}C^{16}O$ + $^{13}C^{16}O$ experiment. The first two appear to track together giving way on final annealing to the 1945.7 $cm^{-1}$ band. These bands are assigned to the $Ti(CO)_5$ and $Ti(CO)_6$ molecules. Titanium hexacarbonyl was prepared, and two broad bands at 1950 and 1987 $cm^{-1}$ were assigned to a distorted $Ti(CO)_6$ molecule in an argon matrix with 10% CO present.[9]

We believe that the strong 1933.5 $cm^{-1}$ argon matrix band with dilute CO (<1%) in argon is due to the isolated $Ti(CO)_6$ molecule and the weaker 1897.7 $cm^{-1}$ band is due to $Ti(CO)_5$. This means that assignments of the higher carbonyl species in the earlier study are incorrect.[10] It now appears that the argon matrix band that grows on annealing at 1964.8 $cm^{-1}$ is due to a metal cluster species, $Ti_x(CO)_y$. The 1769.6 $cm^{-1}$ band, assigned previously to $Ti_2(CO)_2$, appears to be correctly identified.

**$Ti(CO)_x^-$ ($x = 1-6$).** Weak photosensitive bands at 1677.5, 1730.9, 1742.1, 1760.6, 1789.9, 1816.0, 1824.5, and 1861.0 $cm^{-1}$ are almost eliminated by $CCl_4$ doping, so anion species must be considered analogous to the V + CO system. The weak band at 1789.9 $cm^{-1}$ decreased slightly on annealing and disappeared on photolysis using $\lambda > 470$ nm. This band shifts to 1749.5 $cm^{-1}$ in $^{13}C^{16}O$ and 1749.7 $cm^{-1}$ in $^{12}C^{18}O$ spectra and gives the 12/13 ratio 1.0231 and 16/18 ratio 1.0230. The band position and photolysis behavior are in accord with the $TiCO^-$ anion. The $TiCO^-$ anion was calculated to have a $^4\Delta$ ground state with C−O stretching vibration at 1779.8 $cm^{-1}$ and isotopic ratios [(BP86) 12/13: 1.0238, 16/18: 1.0232], and 1834.9 $cm^{-1}$ with isotopic ratios [(B3LYP) 12/13: 1.0234, 16/18: 1.0238]. This is in very good agreement with observed values and supports the anion assignment.

The sharp 1742.1 $cm^{-1}$ band and weak associated band at 1677.5 $cm^{-1}$ decreased on annealing and photolysis using $\lambda > 630$ nm, and disappeared on $\lambda > 470$ nm photolysis. Both bands exhibited carbonyl C−O stretching vibrational isotopic ratios as listed in Table 2. In the mixed $^{12}C^{16}O$ + $^{13}C^{16}O$ experiment, triplets with approximately 1/2/1 relative intensities and matching asymmetries were produced for both bands. These bands are assigned to symmetric and antisymmetric C−O stretching vibrations of the bent $Ti(CO)_2^-$ anion, which is also strongly supported by DFT calculations as listed in Table 4. The stretching modes for the $C_{2v}$ molecule were predicted at 1762.4 and 1718.3 $cm^{-1}$. The symmetric vibration was calculated to be stronger than the antisymmetric vibration, which is also in accord with observations.

Weak bands at 1730.9, 1760.6, 1816.0, 1824.5, and 1861.0 $cm^{-1}$ also show anion behavior following $TiCO^-$ and $Ti(CO)_2^-$; however, in the mixed isotopic experiment, the intermediate components could not be resolved because of band overlap and isotopic dilution. However, these bands show different photolysis behaviors; the 1730.9 $cm^{-1}$ band increased on $\lambda > 470$ nm photolysis when $TiCO^-$ and $Ti(CO)_2^-$ were destroyed, and disappeared on $\lambda > 380$ nm photolysis, while the 1760.6, 1816.0, 1824.5, and 1861.0 $cm^{-1}$ bands increased. This suggests assignment of the 1730.9 $cm^{-1}$ band to $Ti(CO)_3^-$, the 1760.6 $cm^{-1}$ absorption to $Ti(CO)_4^-$, and the 1824.5 and 1861.0 $cm^{-1}$ bands to $Ti(CO)_5^-$ and $Ti(CO)_6^-$, respectively. This photolysis behavior with increasing photon energy required for photodetachment with increasing $x$ for $M(CO)_x^-$ species was observed for Fe, Co, and Ni species in matrix isolation[18−20] and gas-phase studies.[7,35−37]

**$TiCO^+$.** The 2041.3 $cm^{-1}$ band slightly increased on annealing but decreased on $\lambda > 470$ nm photolysis, which photodetached $TiCO^-$. The isotopic frequency ratios (12/13: 1.0225, 16/18: 1.0242) are very close to the diatomic CO ratios. In the mixed $^{12}C^{16}O$ + $^{13}C^{16}O$ experiment, only pure isotopic counterparts were present, so this band involves a single CO submolecule. Of more importance, the 2041.3 $cm^{-1}$ band *increased 4-fold* on $CCl_4$ doping, and this band is assigned to the $TiCO^+$ cation. Our BP86 calculation predicted the C−O stretching mode of $^4\Delta$ ground-state $TiCO^+$ at 2035.4 $cm^{-1}$, which is 5.9 $cm^{-1}$ lower than that observed in solid neon and compares with the predictions for TiCO (32.1 $cm^{-1}$ low) and $TiCO^-$ (10.1 $cm^{-1}$ low). On the other hand, the B3LYP calculation predicted these frequencies 114.4, 52.3, and 45.0 $cm^{-1}$ too high, respectively.

There is no obvious evidence for the $VCO^+$ cation in the neon matrix V + CO system, which was calculated at 2098.5 $cm^{-1}$ by DFT. This cation absorption is probably covered by the strong CO absorption at 2140 ± 10 $cm^{-1}$. The 2116.3 $cm^{-1}$

argon matrix band behaves appropriately for $VCO^+$, but without isotopic data, an assignment cannot be made.

A weaker band at 2057.9 $cm^{-1}$ grows more on annealing than the $TiCO^+$ absorption, and is destroyed by full-arc photolysis. This band might be due to the $Ti(CO)_2^+$ cation, which is calculated to absorb in this region, but we are tentative on such an assignment.

**Other Absorptions.** In the V + CO system, a weak, broad band at 1583.4 $cm^{-1}$ and a sharp band at 1477.9 $cm^{-1}$ increased on annealing, and both bands show C−O stretching vibrational ratios. This region is too low for terminal and bridged carbonyl stretching vibration, so a side-bonded species should be considered. In the mixed $^{12}C^{16}O + {}^{13}C^{16}O$ experiment, doublet was observed for the 1583.4 $cm^{-1}$ absorption, and a 1/2/1 triplet was produced for the 1477.9 $cm^{-1}$ band. These bands are favored in higher power experiments, and are assigned to $V_x$-[CO] and $V_x[CO]_2$ molecules.

**Reaction Mechanisms.** Perhaps the most interesting aspect of this work is that ground-state V and Ti (and Sc)[33] atoms do not react with CO to make the ground-state VCO and TiCO (and ScCO) products, which correlate with low-lying metastable excited atoms of higher spin. The TiCO and ScCO products *do not* increase on annealing, which only gives cold atoms the opportunity to react; reactions (2a, 3a) and the increase in VCO on annealing are rationalized by exposure to the infrared source capable of the atomic excitation in reaction 1b. Reactions (2b, 3b) proceed on ultraviolet−visible photolysis.

$$V(^4F) + CO \xrightarrow{X} VCO\ (^6\Sigma^+) \quad (1a)$$

$$V(^4F) + h\nu\ (IR) \longrightarrow V(^6D) \xrightarrow{CO} VCO(^6\Sigma^+) \quad (1b)$$

$$Ti(^3F) + CO \xrightarrow{X} TiCO\ (^5\Delta) \quad (2a)$$

$$Ti(^3F) + h\nu\ (UV\text{-}VIS) \longrightarrow Ti(^5F) \xrightarrow{CO} TiCO(^5\Delta) \quad (2b)$$

$$Sc(^2D) + CO \xrightarrow{X} ScCO(^4\Sigma^-) \quad (3a)$$

$$Sc(^2D) + h\nu\ (UV\text{-}VIS) \longrightarrow Sc(^4F) \xrightarrow{CO} ScCO \quad (3b)$$

The higher vanadium carbonyls ($x = 2-6$) appear to increase steadily on annealing the solid to 8, 10, and 12 K, but the higher titanium cabonyls ($x = 2-6$) show little growth on 6, 8 K annealing; however, photolysis (visible and ultraviolet) markedly increases the higher titanium carbonyls.

For the carbonyl anions $M(CO)_x^-$ (M = Ti, V, $x = 1-6$) the photodetachment energy increases with $x$ as observed for the Fe, Co, and Ni species in the matrix isolation[18−20] and gas-phase studies.[7,35−37] The $TiCO^-$ and $VCO^-$ anions, for which there are no gas-phase data, show no decrease with $\lambda > 630$ nm but decrease with $\lambda > 470$ nm and decrease more approaching destruction with $\lambda > 380$ nm mercury arc radiation. It appears that both $TiCO^-$ and $VCO^-$ require higher energy radiation for photodetachment than do $FeCO^-$ and $NiCO^-$, with gas-phase thresholds[35−37] measured at 1.26 and 0.80 eV, so the electron affinities of TiCO and VCO should be > 1.3 eV. Although the energies calculated here by DFT for $TiCO^-$ and $VCO^-$ may not be accurate,[38,39] we note that the anions are more stable than TiCO and VCO by 0.91 and 0.64 eV (BP86) and 0.86 and 0.69 eV (B3LYP), respectively.

## Conclusions

Laser-ablated Ti and V atoms were reacted with CO during condensation in excess neon. The metal carbonyl and anion products are identified by isotopic substitution, the effect of $CCl_4$ doping, annealing behavior, and DFT frequency calculations. The major product on deposition with vanadium is $VCO(^6\Sigma^+)$, which arises from the reaction of metastable $V(^6D)$ during deposition; the growth of VCO on annealing requires photoexcitation of ground-state $V(^4F)$ with infrared source radiation. The major product on deposition with titanium is $Ti(CO)_2$ ($^3B_2$) and the low yield of $TiCO(^5\Delta)$ arises from reaction of metastable $Ti(^5F)$ during condensation. Annealing does not increase TiCO, but ultraviolet photolysis, which is capable of exciting Ti, increases TiCO markedly.

Annealing and photolysis increase bands that can be assigned to the higher $M(CO)_x$ ($x = 2-6$) species for both metals. The neon matrix observation for $V(CO)_6$ at 1984.3 $cm^{-1}$ is in excellent agreement with the 1988 $cm^{-1}$ gas-phase value,[29] which suggests that the other neon matrix observations reported here should predict future gas phase observations within 10 $cm^{-1}$. The neon matrix assignment to $Ti(CO)_6$ at 1945.6 $cm^{-1}$ provides a more accurate measurement for $Ti(CO)_6$.

Families of weaker photosensitive bands in the 1870−1670 $cm^{-1}$ region for V and Ti show parallel annealing behavior to the neutral carbonyls and are identified as the corresponding anions $M(CO)_x$ ($x = 1-6$). These bands require increasing energy for photodetachment with increasing $x$, as do the Fe, Co, and Ni carbonyl anions.[18−20]

DFT with the BP86 and B3LYP functionals is extremely useful in predicting the frequencies of these open-shell Ti and V carbonyl species and the $^{13}CO$ and $C^{18}O$ isotopic frequencies (and shifts), although DFT does not calculate accurate atomic energies.[15] The scale factor 0.99 is found for the BP86 pure density functional to predict the frequencies of simple first row molecules,[40] and the five present open-shell TiCO and VCO species require scale factors ranging between 0.993 and 1.017 to fit the neon matrix observations (calculations 13.0 $cm^{-1}$ low to 32.1 $cm^{-1}$ high). On the other hand, the scale factor 0.96 is reported for the hybrid B3LYP functional, and the five triatomic species here require scale factors between 0.947 and 0.975. This and other work[40−45] has shown that the BP86 functional calculates "harmonic" frequencies that reliably approximate observed frequencies and in many cases more closely than the B3LYP functional. Both, however, predict isotopic frequency ratios in agreement with observed values, and provide a description of the normal modes.

**Acknowledgment.** We gratefully acknowledge N.S.F. support for this research under Grant CHE 97-00116.

## References and Notes

(1) Cotton, F. A.; Wilkinson, G. *Advanced Inorganic Chemistry*; Wiley: New York, 1988.

(2) (a) Ford, T. A.; Huber, H.; Koltzbucher, W.; Kundig, E. P.; Moskovits, M.; Ozin, G. A. *Inorg. Chem.* **1976**, *15*, 1666. (b) Hanlan, L.; Huber, H.; Ozin, G. A. *Inorg. Chem.* **1976**, *15*, 2592.

(3) Morton, J. R.; Preston, K. F. *Organometallics* **1984**, *3*, 1386.

(4) Van Zee, R. J.; Bach, S. B. H.; Weltner, W., Jr. *J. Phys. Chem.* **1986**, *90*, 583.

(5) Ishikawa, Y.; Hackett, P. A.; Rayner, D. M. *J. Am. Chem. Soc.* **1987**, *109*, 6644.

(6) Breeze, P. A.; Burdett, J. K.; Turner, J. J. *Inorg. Chem.* **1981**, *20*, 3369.

(7) Sunderlin, L. S.; Wang, D. N.; Squires, R. R. *J. Am. Chem. Soc.* **1993**, *115*, 12060.

(8) McQuaid, M. J.; Morris, K.; Gole, J. L. *J. Am. Chem. Soc.* **1988**, *110*, 5280.

(9) Busby, R.; Klotzbucher, W.; Ozin, G. A. *Inorg. Chem.* **1977**, *16*, 822.

(10) Chertihin, G. V.; Andrews, L. *J. Am. Chem. Soc.* **1995**, *117*, 1595.

(11) Elian, M.; Hoffmann, R. *Inorg. Chem.* **1975**, *14*, 1058.

(12) Burdett, J. K.; *J. Chem. Soc., Faraday Trans.* **1974**, *70*, 1599; *Inorg. Chem.* **1975**, *14*, 375.
(13) Barnes, L. A.; Bauschlicher, C. W., Jr. *J. Chem. Phys.* **1989**, *91*, 314.
(14) Barnes, L. A.; Rosi, M.; Bauschlicher, C. W., Jr. *J. Chem. Phys.* **1990**, *93*, 609.
(15) Fournier, R. *J. Chem. Phys.* **1993**, *99*, 1801.
(16) Adamo, C.; Lelj, F. *J. Chem. Phys.* **1995**, *103*, 10605.
(17) Castro, M.; Salahub, D. R.; Fornier, R. *J. Chem. Phys.* **1994**, *100*, 8233.
(18) Zhou, M. F.; Chertihin, G. V.; Andrews, L. *J. Chem. Phys.* **1998**, *109*, 10893.
(19) Zhou, M. F.; Andrews, L. *J. Phys. Chem. A* **1998**, *102*, 10250.
(20) Zhou, M. F.; Andrews, L. *J. Am. Chem. Soc.* **1998**, *120*, 11499.
(21) Burkholder, T. R.; Andrews L. *J. Chem. Phys.* **1991**, *95*, 8697.
(22) Hassanzadeh, P.; Andrews, L. *J. Phys. Chem.* **1992**, *96*, 9177.
(23) Chertihin, G. V.; Andrews, L. *J. Phys. Chem.* **1995**, *99*, 6356.
(24) Chertihin, G. V.; Bare, W. D.; Andrews, L. *J. Phys. Chem. A* **1997**, *101*, 5090.
(25) Frisch, M. J.; Trucks, G. W.; Schlegel, H. B.; Gill, P. M. W.; Johnson, B. G.; Robb, M. A.; Cheeseman, J. R.; Keith, T.; Petersson, G. A.; Montgomery, J. A.; Raghavachari, K.; Al-Laham, M. A.; Zakrzewski, V. G.; Ortiz, J. V.; Foresman, J. B.; Cioslowski, J.; Stefanov, B. B.; Nanayakkara, A.; Challacombe, M.; Peng, C. Y.; Ayala, P. Y.; Chen, W.; Wong, M. W.; Andres, J. L.; Replogle, E. S.; Gomperts, R.; Martin, R. L.; Fox, D. J.; Binkley, J. S.; Defrees, D. J.; Baker, J.; Stewart, J. P.; Head-Gordon, M.; Gonzalez, C.; Pople, J. A. *Gaussian 94, Revision B.1*; Gaussian, Inc., Pittsburgh, PA, 1995.
(26) (a) Perdew, J. P. *Phys. Rev. B* **1986**, *33*, 8822. (b) Becke, A. D. *J. Chem. Phys.* **1993**, *98*, 5648; Lee, C.; Yang, E.; Parr, R. G. *Phys. Rev. B* **1988**, *37*, 785.
(27) (a) McLean, A. D.; Chandler, G. S. *J. Chem. Phys.* **1980**, *72*, 5639. (b) Krishnan, R.; Binkley, J. S.; Seeger, R.; Pople, J. A. *J. Chem. Phys.* **1980**, *72*, 650.
(28) (a) Wachters, A. J. H. *J. Chem. Phys.* **1970**, *52*, 1033. (b) Hay, P. J. *J. Chem. Phys.* **1977**, *66*, 4377.
(29) Lewis, K. E.; Golden, D. M.; Smith, G. P. *J. Am. Chem. Soc.* **1984**, *106*, 3905.
(30) Darling, J. H.; Ogden, J. S. *J. Chem. Soc., Dalton Trans.* **1972**, 2496.
(31) Burdett, J. K.; Graham, M. A.; Perutz, R. N.; Poliakoff, M.; Rest A. J.; Turner, J. J.; Turner, R. F. *J. Am. Chem. Soc.* **1975**, *97*, 4085.
(32) VanOrden, S. L; Pope, R. M.; Buckner, S. W. *Organometallics* **1991**, *10*, 1089.
(33) Zhou, M. F.; Andrews, L. *J. Phys. Chem. A* **1999**, *103*, 2964.
(34) Poliakoff, M.; Turner, J. J. *J. Chem. Soc., Dalton Trans.* **1973**, 1351.
(35) Engelking, P. C.; Lineberger, W. C. *J. Am. Chem. Soc.* **1979**, *101*, 5569.
(36) Villalta, P. W.; Leopold, D. G. *J. Chem. Phys.* **1993**, *98*, 7730.
(37) Stevens, A. E.; Feigerle, C. S.; Lineberger, W. C. *J. Am. Chem. Soc.* **1982**, *104*, 5026.
(38) Gailbraith, J. M.; Schaefer, H. F., III. *J. Chem. Phys.* **1996**, *105*, 862.
(39) Rösch, N.; Trickey, S. B. *J. Chem. Phys.* **1997**, *106*, 8940.
(40) Scott, A. P.; Radom, L. *J. Phys. Chem.* **1996**, *100*, 16502.
(41) Jonas, V.; Thiel, W. *J. Chem. Phys.* **1995**, *102*, 8474.
(42) Lanzisera, D. V.; Andrews, L. *J. Am. Chem. Soc.* **1997**, *119*, 6392.
(43) Chertihin, G. V.; Andrews, L.; Rosi, M.; Bauschlicher, C. W., Jr. *J. Phys. Chem. A* **1997**, *101*, 9085.
(44) Rosi, M.; Bauschlicher, C. W., Jr.; Chertihin, G. V.; Andrews, L. *Theor. Chem. Acc.* **1998**, *99*, 106.
(45) Zhou, M. F.; Andrews, L. *J. Chem. Phys.* **1999**, *110*, 10370.